

Load spectrum for creep-fatigue life prediction of viewport used in human occupied vehicle

Yiting Kang^{1, 2*}, Yali Feng³, Jinggao Lin⁴, Wenming Zhang¹

¹*School of Mechanical Engineering, University of Science and Technology Beijing, 30 Xueyuan Road, Beijing 100083, China*

²*CONCAVE Research Centre, Department of Mechanical & Industrial Engineering, Concordia University, Montreal, Canada*

³*School of Civil and Environmental Engineering, University of Science and Technology Beijing, 30 Xueyuan Road, Beijing 100083, China*

⁴*China Ocean Mineral Resources Research & Development Association, 1 Fuxingmenwai Street, Beijing 100860, China*

Received 6 September 2014, www.cmnt.lv

Abstract

Acrylic plastic, polymethylmethacrylate (PMMA), are widely employed as the material for the viewports of human occupied vehicle (HOV) which usually dives into deep sea. The service life of viewport is critical to the reliability and safety of HOV. In order to predict life of viewport in design stage, mathematical statistics method is applied to establish the load spectrum for viewport. It is found that ALVIN (America) HOV's dive-depth data is in a skewed distribution, and a piecewise function combined Gumbel and Weibull distributions is proposed for data fitting. HOV undertakes long-term and cyclic load in service, which will cause damage on viewport, so a creep-fatigue load spectrum is established and applied for JIAOLONG (China) HOV's viewport, which integrates both the dive-frequency of each depth range and the duration that maximum stress acts. The proposed method for determination of creep-fatigue load spectrum could thus be considered to be employed for failure analysis and life prediction of modern HOV's viewport.

Keywords: viewport, human occupied vehicle, distribution function, creep and fatigue failure, load spectrum

1 Introduction

Viewport is the main tool to observe and investigate underwater world for scientists and engineers occupied in a HOV. A crucial evaluation standard of a HOV is the number and vision of its viewport. The manned spherical shell of ALVIN HOV (America) has a main viewport and four auxiliary viewports, which can ensure a broad vision in deep sea [1].

Acrylic plastic, PMMA, is the choice material of underwater window rated for depths to 11000m [2]. It is widely employed as the viewport's material due to its optical property, corrosion-resistance, and great strength-weight ratio [3]. The viewport configurations mainly include flat disc, conical frustum, spherical sector, hemisphere, and hyper-hemisphere [4, 5]. HOV need dive to different depths during its service life to finish different scientific investigations, which generates alternating stress and creep strain on viewport due to cyclic and long-term external load [6]. So creep and fatigue are the main failure forms of HOV's viewport [7]. In order to predict its life, a load spectrum for both creep and fatigue analyses should be built at first.

PMMA is a typical viscoelastic material whose fatigue properties are strongly influenced by temperature and cyclic frequency. The creep of PMMA may occur when exposed to the long-term and high load. The creep behaviour of PMMA was theoretically and experimentally investigated by lots of researchers for the characterization, predictive

models, and temperature effect [8-10]. Also its fatigue property is studied for the crack propagation, frequency effect, and life prediction [11-13]. Creep damage accumulates in every cycle with a long time, so the fatigue life is affected by creep. The models for life predicting considering both fatigue and creep effects have been proposed [14, 15]. These works are instructive to future research on life prediction of HOV's viewport. But they cannot be used directly due to the simple structure of PMMA specimen and load spectrum. A comprehensive analysis of creep and fatigue behaviours of PMMA viewport is still lacking. The first step for life prediction is to build a real load spectrum for the viewport.

The dive depth of a HOV for different scientific investigations is a random process about time, so the external load on viewport is also a group of random loads with time span. Mathematical statistics method is applied to analyse dive data to determine the load spectrum of viewport because of the random character of external load.

Professor Sasaki, a Japanese scholar, has made a data statistics on dive frequency of Yomiuri submersible whose maximum dive depth is 300m. Chen [16] has also analysed Yomiuri's data and found an obvious bimodal distribution of dive frequency and depth. Li [17] proposed that Gumbel distribution function can be used to determine fatigue load spectrum of spherical shell used in HOV. Although some studies have been made on load spectrums of submarine and submersible, there are still several problems to be solved. First, a more suitable distribution function should be propo-

*Corresponding author e-mail: kangyiting@sina.com

sed for HOV, which works in deep sea. Second, a load spectrum concerning both time and frequency should be determined for HOV's viewport because its failure behaviour is not only fatigue but also creep.

In this paper, a load spectrum for life prediction of HOV's viewport is determined. Firstly, ALVIN's dive-depth data is collected for analysis and statistics at first. Moreover, Gumbel and Weibull distribution functions are applied for data statistics, and two fitting curves are compared to propose a more suitable function. Finally, the load spectrum for JIAOLONG HOV's viewport is determined based on the new function where both time and frequency are considered.

2 Collection of dive data

The maximum dive-depth of 7 HOVs are more than 4500m, namely MIR I/II and RUS (6000m, Russia), SHINKAI 6500(6500m, Japan), NAUTILE (6000m, France), ALVIN (4500m, America), and JIAOLONG (7000m, China).

The dive-depth data of ALVIN is selected to analyse (Table 1) because it is relatively more comprehensive compared to the others mentioned above. Only total numbers and maximum dive-depth of the others can be found, which is not enough to build a reliable load spectrum.

TABLE 1 Dive data of ALVIN HOV

| Depth range (m) | Frequency | Proportion (%) | Accumulative proportion (%) |
|-----------------|-----------|----------------|-----------------------------|
| 0-300 | 161 | 3.8 | 3.8 |
| 300-600 | 99 | 2.4 | 6.2 |
| 600-900 | 227 | 5.4 | 11.6 |
| 900-1200 | 141 | 3.4 | 15 |
| 1200-1500 | 202 | 4.8 | 19.8 |
| 1500-1800 | 169 | 4.0 | 23.8 |
| 1800-2100 | 377 | 9.0 | 32.8 |
| 2400-2700 | 1311 | 31.2 | 78.2 |
| 2700-3000 | 209 | 5.0 | 83.2 |
| 3000-3300 | 153 | 3.6 | 86.8 |
| 3300-3600 | 137 | 3.3 | 90.1 |
| 3600-3900 | 256 | 6.1 | 96.2 |
| 3900-4200 | 122 | 2.9 | 99.1 |
| 4200-4500 | 38 | 0.9 | 100 |

3 Data fitting of dive-depth

ALVIN's dive data is in an asymmetric and skewed distribution (Figure 1), so Weibull and Gumbel distribution functions are selected for data fitting. The fitting degrees of the two curves are compared to find out a proper function to establish load spectrum of ALVIN.

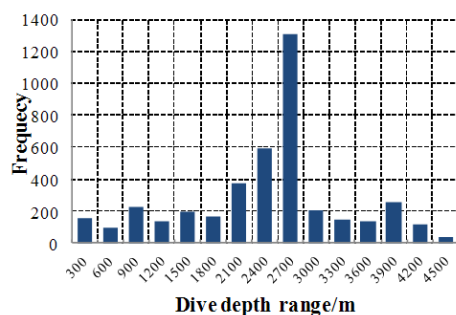


FIGURE 1 Histogram of ALVIN's dive data

3.1 WEIBULL DISTRIBUTION

The frequency distribution with different shapes can be described well by Weibull function with three parameters whose probability density and distribution functions respectively are:

$$f(x) = \frac{\beta}{\eta - \gamma} \left(\frac{x - \gamma}{\eta - \gamma} \right)^{\beta-1} \cdot \exp \left[- \left(\frac{x - \gamma}{\eta - \gamma} \right)^{\beta} \right], \quad (1)$$

$$F(x) = 1 - \exp \left[- \left(\frac{x - \gamma}{\eta - \gamma} \right)^{\beta} \right], \quad (2)$$

where γ is location parameter, β is shape parameter ($\beta > 0$), and η is scale parameter ($\eta > 0$).

It is obvious that location parameter γ of ALVIN's data distribution is 0 according to Figure 1, so only the shape and scale parameters, β and η , are required to be solved. Equations (1) and (2) can be simplified to

$$f(x) = \frac{\beta}{\eta} \left(\frac{x}{\eta} \right)^{\beta-1} \exp \left[- \left(\frac{x}{\eta} \right)^{\beta} \right], \quad (3)$$

$$F(x) = 1 - \exp \left[- \left(\frac{x}{\eta} \right)^{\beta} \right]. \quad (4)$$

The shape and scale parameters could be estimated by graphic method. Firstly, Equation (4) should be transformed by taking the logarithm twice of both the left and right-part:

$$\ln \ln \left(\frac{1}{1 - F(x)} \right) = \beta (\ln x - \ln \eta). \quad (5)$$

Assuming $Y = \ln \ln(1/(1 - F(x)))$, $X = \ln x$ and $B = \beta (\ln \eta)$, Equation (5) can be expressed as:

$$Y = \beta X - B. \quad (6)$$

Obviously, Equation (6) is a line equation, so shape and scale parameters of Weibull distribution, β and η could be obtained from its gradient and intercept.

The confidence intervals of β and B under the confidence level of $1 - \alpha$ are respectively:

$$Q_{\beta} = [\beta - t_{1-\frac{\alpha}{2}}(n-2) \cdot \sigma_{\beta}, \beta + t_{1-\frac{\alpha}{2}}(n-2) \cdot \sigma_{\beta}], \quad (7)$$

$$Q_B = [B - t_{1-\frac{\alpha}{2}}(n-2) \cdot \sigma_B, B + t_{1-\frac{\alpha}{2}}(n-2) \cdot \sigma_B]. \quad (8)$$

3.2 GUMBEL DISTRIBUTION

Gumbel function is a theoretical model whose extreme value is in asymptotic distribution, and its probability density function and distribution function respectively are:

$$f(x) = \frac{1}{\varphi} \cdot \exp \left[\frac{x - \lambda}{\varphi} - \exp \left(\frac{x - \lambda}{\varphi} \right) \right], \quad (9)$$

$$F(x) = 1 - \exp \left[-\exp \left(\frac{x - \lambda}{\varphi} \right) \right], \quad (10)$$

where φ is shape parameter ($\varphi > 0$), and λ is scale parameter.

The shape and scale parameters of Gumbel distribution can also be obtained by transforming Equation (10) to:

$$\ln \ln \left(\frac{1}{1 - F(x)} \right) = \frac{1}{\varphi} (x - \lambda). \quad (11)$$

Assuming $Z = \ln \ln(1/(1 - F(x)))$, $C = 1/\varphi$ and $D = \lambda/\varphi$, Equation (11) can be also transformed to a line equation:

$$Z = Cx + D. \quad (12)$$

So the shape and scale parameters of Gumbel distribution, φ and λ , could be solved from the gradients and intercept of Equation (12).

The confidence intervals of C and D under the confidence level of $1 - \alpha$ are respectively:

$$Q_C = [C - t_{1-\frac{\alpha}{2}}(n-2) \cdot \sigma_C, C + t_{1-\frac{\alpha}{2}}(n-2) \cdot \sigma_C], \quad (13)$$

$$Q_D = [D - t_{1-\frac{\alpha}{2}}(n-2) \cdot \sigma_D, D + t_{1-\frac{\alpha}{2}}(n-2) \cdot \sigma_D]. \quad (14)$$

3.3 COMPARISON OF CURVES FITTED USING WEIBULL AND GUMBEL DISTRIBUTION

Curve of ALVIN's dive data fitted employing Weibull distribution is shown in Figure 2, which indicates that the fitting degree is much higher when the dive-depth is over 2700m. β and η are solved ($\beta=3.1059$, and $\eta=2599.2$), so the distribution function can be obtained

$$f(x) = \frac{3.1059}{2599.2} \left(\frac{x}{2599.2} \right)^{2.1059} \cdot \exp \left[-\left(\frac{x}{2599.2} \right)^{3.1059} \right], \quad (15)$$

$$F(x) = 1 - \exp \left[-\left(\frac{x}{2599.2} \right)^{3.1059} \right]. \quad (16)$$

The curve fitted by Gumbel distribution is also shown in Figure 2, which suggests it agrees well with the origin data when the dive depth is less than 2700m. φ and λ are solved ($\varphi = 725.42$, and $\lambda = 2634.6$), so the distribution function can be obtained:

$$f(x) = \frac{1}{725.42} \exp \left[\frac{x - 2634.6}{725.42} - \exp \left(\frac{x - 2634.6}{725.42} \right) \right], \quad (17)$$

$$F(x) = 1 - \exp \left[-\exp \left(\frac{x - 2634.6}{725.42} \right) \right]. \quad (18)$$

Q_β and Q_B in Weibull distribution under the confidence level of 80% are [1.2985, 1.7366] and [8.5725, 12.9942]. Q_C and Q_D in Gumbel distribution under the confidence level of 95% are [0.0009, 0.0011] and [-2.9553, -2.5156].

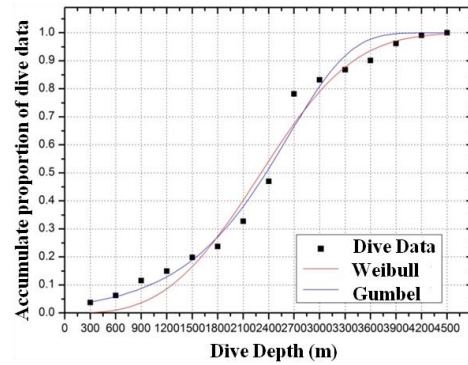


FIGURE 2 Comparison of two curves fitted by Weibull and Gumbel

When dive depth (x) is less than 2700m, fitting degree of the curve "Gumbel" is much better, while that of "Weibull" is superior when x is more than 2700m. So distribution function can be expressed with the combination of Gumbel and Weibull:

$$F(x) = \begin{cases} 1 - \exp \left[-\exp \left(\frac{x - 2634.6}{725.42} \right) \right], & x < 2700 \\ 1 - \exp \left[-\left(\frac{x}{2599.2} \right)^{3.1059} \right], & x \geq 2700 \end{cases}. \quad (19)$$

Dive frequency (n) of ALVIN in the depth-range $[d_1, d_2]$ can be solved by:

$$n = \begin{cases} N \{ \exp[-\exp(\zeta_1)] - \exp[-\exp(\zeta_2)] \}, & x < x_p \\ N \{ \exp[-(\xi_1)^{3.1059}] - \exp[-(\xi_2)^{3.1059}] \}, & x \geq x_p \end{cases}, \quad (20)$$

where N is the total dive frequency, $\zeta_i = \frac{d_i - 2634.6}{725.42}$,

$\xi_i = \frac{d_i}{2599.2}$, $i = 1, 2$ and $x_p = 2700$.

Result of n solved by Equation (20) is shown in Table 2, which clearly demonstrates Weibull and Gumbel are respectively applicable for data fitting in different depth-ranges. And it is necessary to develop a new function with the combination of Weibull and Gumbel.

TABLE 2 Dive data of ALVIN solved by Weibull and Gumbel functions

| No. | Depth-range (m) | Frequency | Proportion (%) | | |
|-----|-----------------|-----------|----------------|---------|--------|
| | | | Real | Weibull | Gumbel |
| 1 | 0-300 | 161 | 3.8 | 0.1 | 3.9 |
| 2 | 300-600 | 99 | 2.4 | 0.9 | 1.9 |
| 3 | 600-900 | 227 | 5.4 | 2.6 | 2.9 |
| 4 | 900-1200 | 141 | 3.4 | 5.0 | 4.2 |
| 5 | 1200-1500 | 202 | 4.8 | 7.9 | 6.0 |
| 6 | 1500-1800 | 169 | 4.0 | 10.8 | 8.2 |
| 7 | 1800-2100 | 377 | 9.0 | 12.9 | 10.9 |
| 8 | 2100-2400 | 595 | 14.2 | 13.9 | 13.5 |
| 9 | 2400-2700 | 1311 | 31.2 | 13.4 | 15.0 |
| 10 | 2700-3000 | 209 | 5.0 | 11.5 | 14.4 |
| 11 | 3000-3300 | 153 | 3.6 | 8.7 | 10.9 |
| 12 | 3300-3600 | 137 | 3.3 | 5.9 | 5.9 |
| 13 | 3600-3900 | 256 | 6.1 | 3.5 | 1.9 |
| 14 | 3900-4200 | 122 | 2.9 | 1.8 | 0.3 |
| 15 | 4200-4500 | 38 | 0.9 | 0.8 | 0.0 |

The sum of squares of the difference between fitting results and real data are:

$$E_j = \sum_{i=1}^{15} (P_{ji} - P_i)^2, \quad j = W, G, P, \quad (21)$$

where P_{ji} and P_i are respectively the fitting result and real value in No. i depth-range, and subscript j indicates the different fitting curves: W (Weibull distribution), G (Gumbel distribution), and P (combined both W and G). E_W , E_G and E_P are listed in Table 3. Values of E_W and E_G are almost equal, however that of E_P is much smaller comparing to E_W and E_G . The distribution equations combined both Weibull and Gumbel is more effective for data fitting of dive-depth.

TABLE 3 Sum of squares of difference between fitting result and real data

| Parameter Value | E_W | E_G | E_P |
|-----------------|----------|----------|----------|
| | 0.049733 | 0.046639 | 0.037577 |

4 Load spectrum for viewport of JIAOLONG HOV

Based on the above analysis of ALVIN's dive data, a piecewise function, which combines Gumbel and Weibull distributions is selected to determine the load spectrum of viewports used in JIAOLONG HOV for creep and fatigue analysis.

Maximum dive-depth of JIAOLONG is 7000m, which is greater than that of ALVIN, so the independent variable in Equation (11) should be transformed to get the new distribution function:

$$F(x) = \begin{cases} 1 - \exp \left[-\exp \left(\frac{4.5x/7 - 2634.6}{725.42} \right) \right], & x < 4200 \\ 1 - \exp \left[-\left(\frac{4.5x/7}{2599.2} \right)^{3.1059} \right], & x \geq 4200 \end{cases}, \quad (22)$$

Dive frequency n of JIAOLONG in the depth-range $[d_1, d_2]$ can be calculated by:

$$n = \begin{cases} N \left\{ \exp \left[-\exp(\zeta_1) \right] - \exp \left[-\exp(\zeta_2) \right] \right\}, & x < x_p \\ N \left\{ \exp \left[-(\xi_1)^{3.1059} \right] - \exp \left[-(\xi_2)^{3.1059} \right] \right\}, & x \geq x_p \end{cases}, \quad (23)$$

where $\zeta_i = \frac{4.5d_i/7 - 2634.6}{725.42}$, $i = 1, 2$, $\xi_i = \frac{4.5d_i/7}{2599.2}$, $x_p = 4200$, and d_1 and d_2 are between 0 and 7000m.

The data of JIAOLONG's viewport in every depth-range solved by Equation (23) are listed in Table 4.

The fatigue load spectrum of JIAOLONG when it finishes a dive to 7000m is shown in Figure 3.

When JIAOLONG HOV serves, both creep and fatigue damages may occur on its viewports because of the effect of alternating load and long-term load. Creep is a time dependent structural behaviour of acrylic. As a result, the duration of external load should be taken into account in the establishment of its load spectrum. In normal conditions, underwater time of HOV does not exceed 8 hours, and diving and floating speed are about 40m/min. So the duration that maximum stress acts is:

$$t = 8 - \frac{x}{1200}. \quad (24)$$

TABLE 4 Dive data of JIAOLONG HOV (a depth-range: 500m)

| No. | Depth-range (m) | Frequency | Proportion (%) |
|-----|-----------------|-----------|----------------|
| 1 | 0-500 | 5 | 3.9 |
| 2 | 500-1000 | 2 | 1.9 |
| 3 | 1000-1500 | 4 | 2.9 |
| 4 | 1500-2000 | 5 | 4.2 |
| 5 | 2000-2500 | 8 | 6 |
| 6 | 2500-3000 | 10 | 8.2 |
| 7 | 3000-3500 | 14 | 10.9 |
| 8 | 3500-4000 | 17 | 13.5 |
| 9 | 4000-4500 | 19 | 15 |
| 10 | 4500-5000 | 11 | 8.7 |
| 11 | 5000-5500 | 7 | 5.9 |
| 12 | 5500-6000 | 4 | 3.5 |
| 13 | 6000-6500 | 2 | 1.8 |
| 14 | 6500-7000 | 1 | 0.8 |

Load spectrum considering both the dive frequency and duration that maximum stress acts for creep and fatigue analysis and life prediction of JIAOLONG HOV's viewports is illustrated in Figure 4 and Table 5.

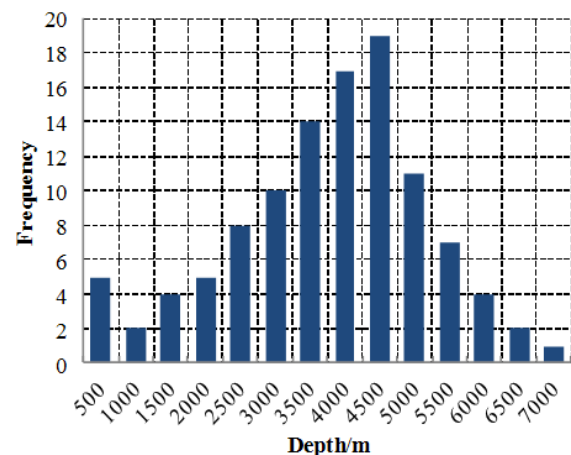


FIGURE 3 Fatigue load spectrum of JIAOLONG HOV

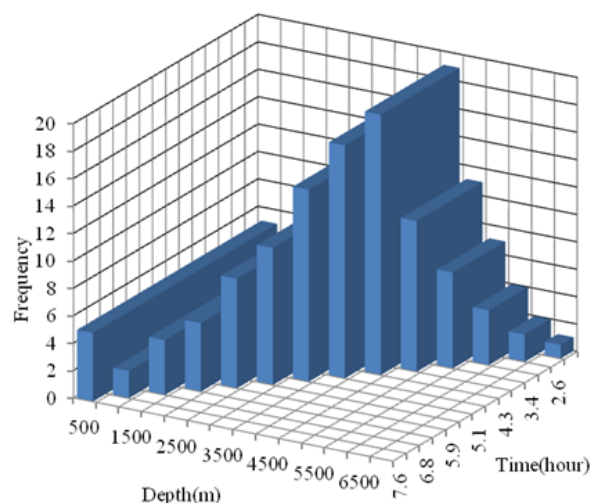


FIGURE 4 Creep and fatigue load spectrum of JIAOLONG HOV

TABLE 5 Data in creep-fatigue load spectrum of JIAOLONG HOV

| Depth-range (m) | Frequency | Proportion (%) | Duration (h) |
|--------------------|-----------|-------------------|-----------------|
| 0-500 | 5 | 3.9 | 7.6 |
| 500-1000 | 2 | 1.9 | 7.2 |
| 1000-1500 | 4 | 2.9 | 6.8 |
| 1500-2000 | 5 | 4.2 | 6.3 |
| 2000-2500 | 8 | 6 | 5.9 |
| 2500-3000 | 10 | 8.2 | 5.5 |
| 3000-3500 | 14 | 10.9 | 5.1 |
| 3500-4000 | 17 | 13.5 | 4.7 |
| 4000-4500 | 19 | 15 | 4.3 |
| 4500-5000 | 11 | 8.7 | 3.8 |
| 5000-5500 | 7 | 5.9 | 3.4 |
| 5500-6000 | 4 | 3.5 | 3.0 |
| 6000-6500 | 2 | 1.8 | 2.6 |
| 6500-7000 | 1 | 0.8 | 2.2 |

5 Conclusions

In order to determine a load spectrum for failure analysis of viewport used in JIAOLONG HOV, dive data of ALVIN

References

- [1] Lin J, Feng Y, Zhang W, Kang Y 2013 Review on Viewport Used in Human Occupied Vehicle *Ship Engineering* **35**(3) 1-5 (in Chinese)
- [2] Stachiw J D 1970 Conical Acrylic Windows under Long Term Hydrostatic Pressure of 20,000 psi *Journal of Engineering for Industry* **92**(1) 237-56
- [3] Stachiw J D 2004 Acrylic plastic as structural material for underwater vehicles *International Symposium on Underwater Technology* 289-96
- [4] American National Standard American Society of Mechanical Engineers *Safety Standard for Pressure Vessels for Human Occupancy* PVHO-1 1977 (www.asme.org, Codes and Standards)
- [5] Stachiw J D 2003 Handbook on Acrylics for Submersibles, Hyperbaric Chambers, and Aquaria *Best Publishing Company: Flagstaff*
- [6] Stachiw J D 1976 Spherical Shell Sector Acrylic Plastic Windows with 12,000 ft Operational Depth for Submersible ALVIN *Journal of Engineering for Industry* **98**(2) 523-36
- [7] Lin J, Zhang W, Feng Y, and Kang Y 2013 Displacement and Stress Analysis of Viewport Used in Human Occupied Vehicle Based on Rayleigh-Ritz *Journal of Ship Mechanics* **17**(6) 635-44
- [8] Arnold J C and White V E 1995 Predictive models for the creep behaviour of PMMA *Material Science and Engineering* **197**(2) 251-60
- [9] Gao Z Z, Liu W, Liu Z Q, and Yue, Z F 2010 Experiment and Simulation Study on the Creep Behavior of PMMA at Different Temperatures *Poly-Plastics Technology and Engineering* **49**(14) 1478-82
- [10] Chen K, and Hsu R 2007 Evaluation of environmental effects on mechanical properties and characterization of creep behavior of PMMA *Journal of the Chinese Institute of Engineers* **30**(2) 267-74
- [11] Carnelli D, Villa T, Gastaldi D, and Pennati G 2011 Predicting fatigue life of a PMMA based knee spacer using a multiaxial fatigue criterion *Journal of Applied Biomaterials and Biomechanics* **9**(3) 185-92
- [12] Hoey D, and Taylor D 2009 Comparison of the fatigue behaviour of two different forms of PMMA *Fatigue and Fracture of Engineering Materials and Structures* **32**(3) 261-9
- [13] Huang A, Yao W, and Chen F 2014 Analysis of Fatigue Life of PMMA at Different Frequencies Based on a New Damage Mechanics Model *Mathematical Problems in Engineering* Article ID 352676 1-8
- [14] Hu Y, Summers J, Hiltner A, Baer E 2003 Correlation of fatigue and creep crack growth in poly(vinyl chloride) *Journal of Materials Science* **38**(4) 633-42
- [15] Liu W, and Yang X J 2012 Damage evolution with growing cyclic creep and life prediction of MDYB-3 PMMA *Fatigue and Fracture of Engineering Materials and Structures* **36**(6) 483-91
- [16] Chen X 1994 Low-cycle fatigue of submarine and submersible *National Defence Industry Press: Beijing (in Chinese)*
- [17] Li X, Liu T, Huang X, and Cui W 2004 Determination of fatigue load spectrum for pressure hull of a deep manned submersible *Journal of Ship Mechanics* **8**(1) 59-70

HOV (America) is collected for analysis and statistics due to its completeness and comparability. It has been found that the dive data has a skewed distribution feature, so both Weibull and Gumbel distributions are selected and compared for ALVIN's data fitting. The results indicate that Weibull and Gumbel function are respectively suitable for fitting data of different depth-ranges, so a piecewise distribution function is proposed to determine the load spectrum with the combination of two distribution functions. Both creep and fatigue are the main failure forms for HOV's viewport made by PMMA, so a load spectrum concerning dive time and frequency, which can be used for, creep and fatigue analysis is determined for JIAOLONG's viewport at last.

Acknowledgements

The authors gratefully acknowledge the support of National High-tech R&D Program (863 Program, 2011AA09A101).

Authors



Yiting Kang, born in September, 1986, Anhui Province, P.R. China

Current position, grades: postdoctoral Fellow at the CONCAVE Research Centre, Department of Mechanical & Industrial Engineering, Concordia University, Canada.

University studies: Doctoral Degree in Vehicle Engineering from University of Science and Technology Beijing in China.

Scientific interests: vehicle dynamics and kinematics of vehicle suspension.

Publications: more than 10 papers.

Experience: 3 scientific research projects.



Yangli Feng, born in September, 1967, Beijing, P.R. China

Current position, grades: professor at the School of Civil and Environmental Engineering, University of Science and Technology Beijing, China.

University studies: Doctoral Degree Vehicle Engineering from University of Science and Technology Beijing in China.

Scientific interests: equipment for mining resource development, optimization and control of mineral processing, and mineral microorganism technology.

Publications: more than 100 papers.

Experience: teaching experience of 24 years, more than 10 scientific research projects.

| | |
|---|---|
|  | <p>Jinggao Lin, born in April, 1986, Liaoning Province, P.R. China</p> <p>Current position, grades: engineer at the China Ocean Mineral Resources Research & Development Association.</p> <p>University studies: doctoral degree Vehicle Engineering from University of Science and Technology Beijing in China.</p> <p>Scientific interest: creep and fatigue analyses of HOV's viewports.</p> <p>Publications: 5 papers.</p> <p>Experience: in 3 scientific research projects.</p> |
|  | <p>Wenming Zhang, born in August, 1955, Beijing, P.R. China</p> <p>Current position, grades: professor at the School of Mechanical Engineering, University of Science and Technology Beijing, China.</p> <p>University studies: Master Degree in Vehicle Engineering from University of Science and Technology Beijing in China.</p> <p>Scientific interest: design and development of heavy duty mining truck and handling and ride performance analyses of off-highway vehicle.</p> <p>Publications: more than 100 papers.</p> <p>Experience: teaching experience of 30 years, more than 10 scientific research projects.</p> |